Alkaline Extraction of Alumina from Hydrogen Reduced Bauxite Residue Pellets

Georgia-Maria Tsaousi[1], Michail Vafeias[2], Adamantia Lazou[3], Dimitrios Sparis[4], Dimitrios Kotsanis[5], Efthymios Balomenos[6] and Dimitrios Panias[7]
1. Senior Researcher
2. Supervising Researcher
3. Post-Doc Researcher
4. PhD Researcher
5. Materials Characterization specialist
6. Assistant Professor
7. Professor of Extractive Metallurgy, Head of Research Group
Technologies for Sustainable Metallurgy, Laboratory of Metallurgy, NTUA, Athens, Greece
Corresponding author: margitsaousi@metal.ntua.gr
https://doi.org/10.71659/icsoba2024-br008

Abstract

Several process alternatives are being investigated for the use of bauxite residue (BR) as a secondary metallurgical resource. These processes aim primarily at the extraction of the major metal values found in BR, i.e., Fe, Al and Na, and attempt to integrate novel metallurgical technologies to reduce the CO_2 footprint. One of these technologies is the reduction of BR with H_2 for the production of Fe, taking place in a temperature range below the melting point of Fe. In this process, the remaining unreduced oxides contain the Al content of BR in aluminate phases which need to be leached efficiently. In this paper, hydrogen reduced pellets of BR/CaO mixtures are being hydrometallurgically treated to leach the alumina content. The pellets are first chemically and physically characterized. The main challenges identified are (i) the entrapment of Fe in the oxide matrix and (ii) the formation of unleachable aluminate phases. Two approaches were tested in an attempt to assess the optimum way of separating the Fe content of the pellets and the efficient leaching of the aluminate phases: (a) an "alkaline leaching stage first/Fe separation second" approach, in which standard leaching tests are first performed with a Na_2CO_3 solution to separate the Fe from the leaching residue and (b) a "Fe separation first/alkaline leaching second" approach, where the pellets were smelted to separate pyrometallurgically the Fe content from the aluminate phases and then leaching was performed with a Na_2CO_3 solution. Results indicate that the second process route is more efficient for the separation of Fe.

Keywords: Hydrogen Reduction, Alumina leaching, Iron separation.

1. Introduction

Bauxite residue (BR) is an industrial by-product generated during the production of alumina from bauxite ores in the Bayer process. The current BR production level in the EU is 6.8 Mtpa (million tonnes per year); while the cumulative stockpiled level is a staggering > 250 Mt (dry matter). According to the International Aluminium Institute (IAI) Bauxite Residue (BR) production annually is approximately 170 Mt, while 8 Gt of bauxite residue will be stored globally by 2040, as the residue must be unavoidably landfilled [1].

BR is rich in metal oxides of e.g., Fe, Al, Ti, in addition, certain BR qualities contain reasonably high levels of rare-earth elements (REEs). BR is, therefore, an interesting potential resource for several metals, iron being the most attractive [2─4]. The processes explored for the extraction of Fe from BR typically involve reduction smelting in an EAF, with carbon being used as the reductant. Consequently, the reductive smelting of BR to produce pig-iron and slag is an energy-

intensive process that involves high-temperature melting (> 1300 °C) and is associated with a substantial environmental footprint [5, 6].

In this study, Fe separation from BR is proposed through a hydrogen-reduction process by an innovative metallurgical technology developed in the framework of the HARARE EU Horizon project [7]. The HARARE technology aims to validate the use of hydrogen as a reductant in the metallurgical sector as it has the biggest decarbonization potential and is therefore the most compatible option with the EU's climate neutrality goal and the decarbonization of Europe's economy [8]. The use of hydrogen in the production of Fe from its oxides allows, theoretically, for the reduction to take place in the solid state (below the melting point of the system), eliminating the need to melt the BR, and saving large amounts of energy. Moreover, using BR as a raw material decreases the raw material costs of the process.

The yield and recovery of Fe is dependent on the reduction conditions and the fluxing (chemistry) of the BR agglomerates, as well as the rate and extent of the reduction reactions and simultaneous sintering phenomena. The main challenge is to optimize the agglomeration and hydrogen reduction conditions to obtain high metal recovery in the separation, which is beneficial for the subsequent stage of alumina recovery. Thus, the second target of the process is the production of a non-metallic fraction which is predominantly of calcium aluminate composition. This easily leachable in Na_2CO_3 solutions alumina-containing fraction (slag) is a feedstock for alumina production [9]. For this reason, CaO is used as the main fluxing agent.

In this study, a sample of material produced after the laboratory hydrogen reduction of BR/CaO pellets (termed "H_2 reduced pellets") was characterized and tested for the leaching of Al. As the reduced pellets have not been subjected to any Fe separation process, a second goal of this work was to assess how the state of the Fe (particle size and morphology) might affect the hydrometallurgical process. Two approaches are presented: (a) an alkaline leaching stage first/Fe separation second approach, and (b) a Fe separation first/ alkaline leaching second approach. In the first approach, a standard leaching test is first performed on the reduced pellets with a Na_2CO_3 solution and then the separation of Fe from the leaching residue by magnetic separation is evaluated. In the second approach, the reduced pellets are smelted to pyrometallurgically separate the Fe content from the aluminate phases and then leaching is performed with a Na_2CO_3 solution.

2. Materials and Methods

2.1 Equipment and Instruments Used

The leaching tests were conducted inside a custom-made reactor. The body of the reactor (heating mantle, stirring unit and vessel) was built from parts of a Parr™ 4563 model. The vessel had a maximum volume of 0.6 L and was made from Inconel alloy. The reactor lid was replaced by a custom-made PTFE lid, suitable for leaching tests at atmospheric pressure. The lid was constructed with suitable sockets which allowed for: (a) attaching a vapor condenser, (b) the immersion of a thermocouple and a mechanical stirrer (c) the insertion of the solid sample. Heating and stirring were controlled by an external PLC unit.

Elemental chemical analysis of the aqueous samples was performed with a PerkinElmer™ PinAAcle 900 T Atomic Absorption Spectrometer (AAS) and a PerkinElmer™ Optima 800 Optical Emission Spectrometer (ICP-OES). Crystallographic analysis of the solid samples was performed in a Miniflex600 Rigaku diffractometer, with CuKα radiation (V = 40 kV and I = 15 mA). Phase identification was performed with Bruker™ Diffrac EVA software and use of ICDD™ Diffraction databases PDF-4+ 2023 and PDF-4 Minerals 2023 [10]. Particle size analysis was performed with a Horiba Partica LA-960 V2 laser scattering particle size distribution

analyzer. The microstructure study of the materials was performed using a JEOL6380LV scanning electron microscope.

2.2 Materials Used

The H_2 reduced pellets were crushed and ground until the material passed through the 180 µm sieve. Sampling of the ground pellets was conducted using a Jones rifle splitter. Samples were drawn for chemical, crystallographic, microscopic and particle size analysis. For the chemical analysis of the ground pellets and the leach residues, dry samples were fused with a mixture of $Li_2B_4O_7$ (≥ 99.9 % trace metals basis) and $LiBO_2$ (≥ 99.9 % trace metals basis) and the melt was dissolved in 10 % HNO_3 solution. After complete dissolution, liquid samples were taken and analyzed by AAS and ICP-OES. The chemical analysis of the H_2 reduced pellets (in equivalent oxide basis) is shown in Table 1.

Table 1. Chemical analysis of the H_2 reduced pellets used in this research work.

Oxide	Al_2O_3	SiO_2	CaO	Na_2O	TiO_2	Fe total	Others
Composition (% (w/w))	20.6 ± 0.24	9.4 ± 0.09	36.5 ± 1.34	2.9 ± 0.09	3.9 ± 0.02	23.5 ± 0.34	1.94

The results reveal high CaO, Al_2O_3 and Fe content, as expected, since the raw material had not been previously subjected to any Fe separation method. Figure 1 shows the X-Ray Diffractogram of the H_2 reduced pellets.

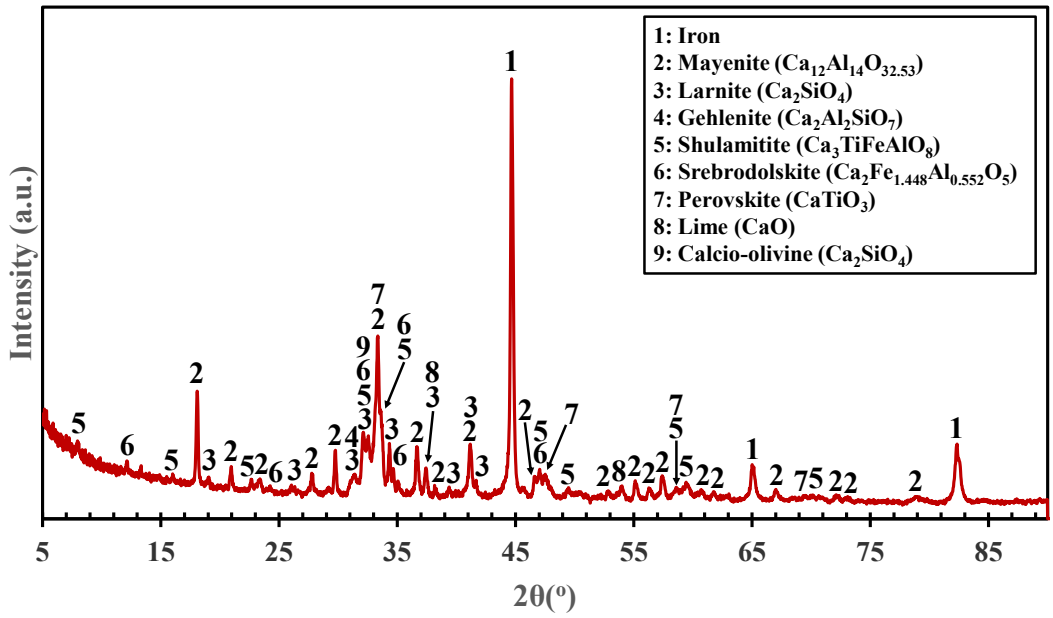

Figure 1: Powder X-Ray Diffractogram and phase identification of the H_2 reduced pellets used in this research work.

The H_2 reduced pellets are a mixture of metallic Fe with several calcium aluminate, silicate and mixed aluminate/silicate oxides. In more detail, mayenite is the only calcium aluminate phase formed, while two polymorphs of dicalcium silicate (larnite and calcio-olivine) are observed. Gehlenite is also present in the non-metallic fraction, which is a mixed Ca-Al-silicate. TiO_2 is observed in perovskite and the perovskite-related phase of shulamitite. Minor compounds observed include some unreacted lime (CaO). In terms of leachability in Na_2CO_3 solution, the mayenite is expected to be the major contributor to Al extraction. Gehlenite is practically

unleachable in Na_2CO_3 solutions. Consequently, high Al extraction rates from the direct leaching of the pellets should not be expected.

The ground H_2 reduced pellets were also examined for their particle size distribution by Horiba Partica LA-960 V2 laser analyzer based on dry-powder dispersion method (compressed air dispersion using Venturi). The results indicated that the ground material was extremely fine, with D(0.5) = 9.57 µm, and D(0.9) = 68.28 µm. This is an indication that both the metallic and non-metallic fraction of the material is extremely fine, which could pose challenges in any magnetic separation process. To verify this observation a microscopic analysis of the material was also performed, and the results are presented in Figure 2 below.

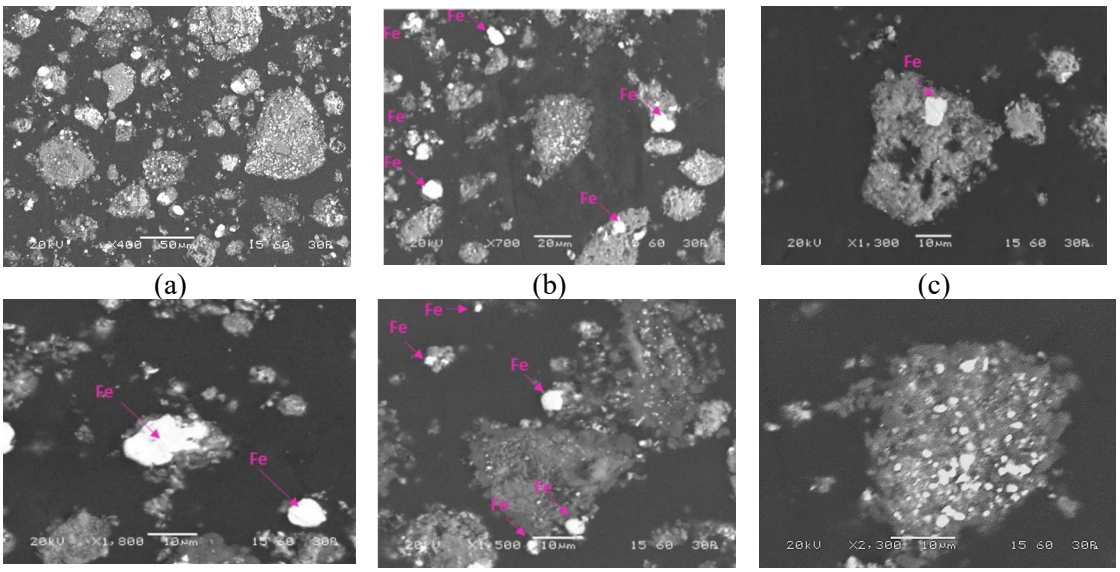

(a) (b) (c)

(d) (e) (f)

Figure 2. Scanning Electron Microscopy images of H_2 reduced pellets at different magnification levels.

The microscopic analysis of the H_2 reduced pellets sample (Figure 2, (a)–(f)) confirms the previous hypothesis about the particle size of the metallic (Fe) fraction. The bright white particles were identified as metallic iron, while the gray areas represent the non-metallic fraction matrix. Indeed, the particle size is fine, with particle diameters ranging from 1–14.2 µm. In addition, it is observed that the Fe content of the pellets is finely distributed and locked in the non-metallic fraction matrix [11, 12].

2.3 Experimental Methodology

As described earlier, two approaches were studied in this work: (a) an alkaline leaching first/Fe separation second approach, and (b) a Fe separation first/alkaline leaching second approach. The methodologies followed are described in separate sections below.

2.3.1 Alkaline Leaching First/Fe Separation Second Approach

In this approach (Figure 3) a standard leaching test was performed on the H_2 reduced pellets and then Fe separation was attempted by magnetic separation from the leaching residue (also termed Grey Mud).

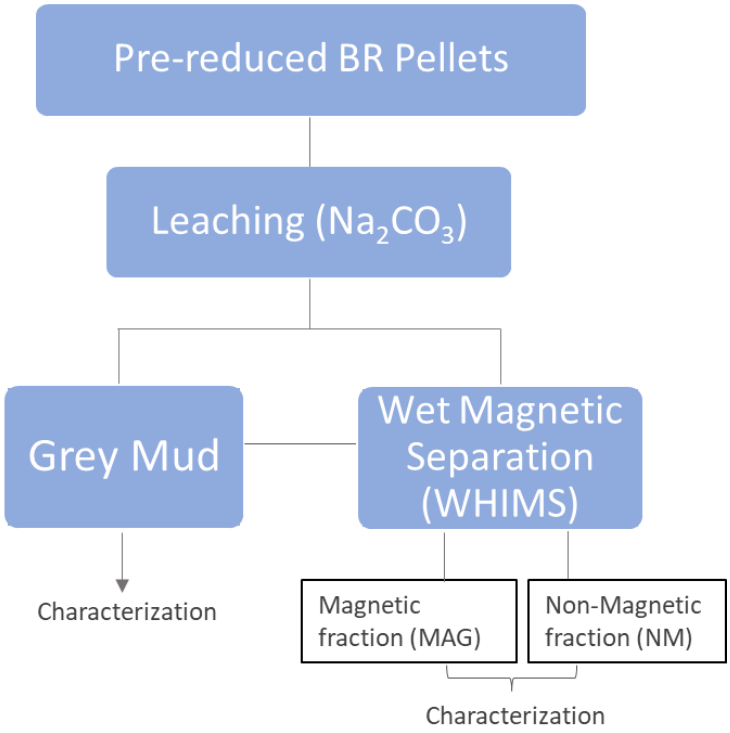

Figure 3. Flowsheet of Alkaline leaching first/Fe separation second approach.

For the leaching study an 8 % (w/w) aqueous Na_2CO_3 solution was chosen as the leaching solution (corresponding to 86.5 g Na_2CO_3/L, calculated based on the density of 8 % (w/w) Na_2CO_3 at 20 °C which is equal to 1.0816 g/cm^3) [13]. The choice is based on previous published work [14]. The leaching solution was prepared by deionized H_2O and reagent grade Na_2CO_3 (≥ 99.5 %, ACS reagent). For the leaching tests, 0.3 L of the solution was transferred to the reactor and preheated to the temperature selected for each test. After sealing the reactor, mechanical stirring was applied at a rate of 300 rpm (vigorous stirring). Ground H_2 reduced pellets were added to the reactor when the set temperature was stabilized to ± 2 °C. The timer was started at this point and at the end of the leaching the slurry was removed and filtered with a Buchner funnel. The liquor, and washed and dried (for 24 h, at 105 °C) residue were sent for analysis by AAS and ICP required for the calculation of the leaching efficiency and characterization of the leach residue by XRD.

The experimental conditions of the H_2 reduced pellets leaching are summarized in Table 2. The selected S/L ratio corresponds to a 20 % molar excess of CaO compared to the moles of Na_2CO_3 (i.e. moles CaO/moles Na_2CO_3 = 1.2). This value has been used in the leaching of similar materials from our group, along with the temperature and duration values of the trial.

Table 2. Experimental conditions of H_2 reduced pellets leaching tests performed in this research work.

Duration (h)	6
S/L ratio (%)	14.38
Na_2CO_3 (wt. %)	8
Excess of H_2 reduced pellets (%)	20
Temperature (°C)	95
Stirring rate (rpm)	300

After leaching, the residue of the process was washed and dried for 24 h. Then, a sample of the residue was subjected to wet magnetic separation (using a CarpcoTM Wet High Intensity Magnetic Separator-WHIMS) to assess the potential of Fe separation from the material.

2.3.2 Fe Separation First/Alkaline Leaching Second Approach

With this approach, the goal is to separate the Fe by smelting and create a slag that will be used for the subsequent hydrometallurgical extraction work.

First, thermochemical simulations were implemented with the use of FactSage 8.3 [15] software to analyze a) the interaction of slag and metal at equilibrium, b) the phase assemblage, c) the composition of slag and alloy, and d) the liquidus of the slag. A simplified version of the H_2 reduced pellets chemical composition (Table 1) was used as input for the calculations. The oxide solid and liquid solutions were described by the FToxide database, and the FSstel was used to estimate the liquid metal (Liquid), pure substances, and gas species were described by the FactPS database. According to the results (Figure 4), theoretical melting point was determined at 1642 °C and the first phase precipitating upon cooling was b-Ca_2SiO_4.

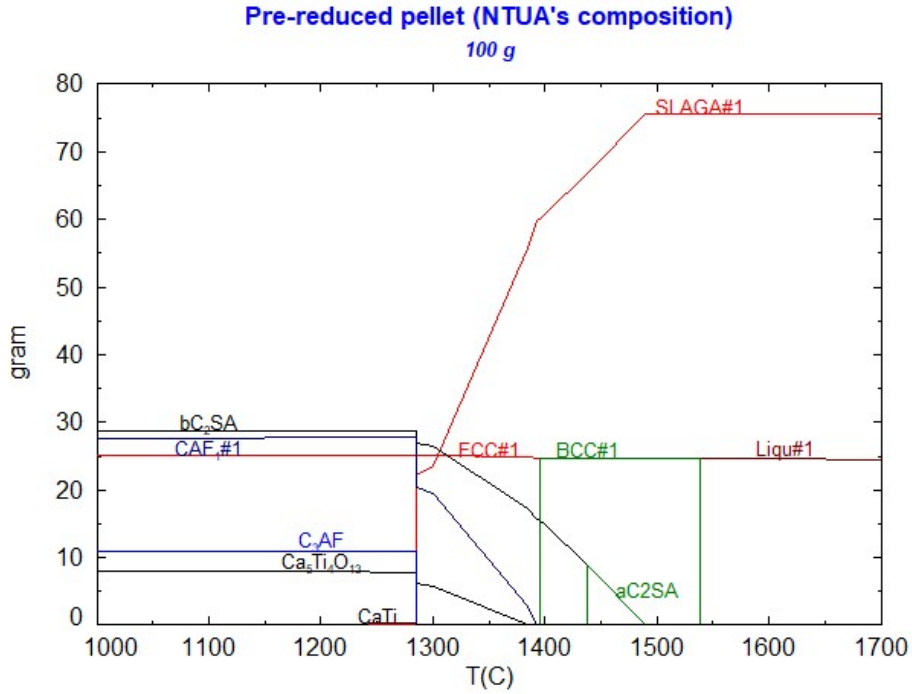

Figure 4. Thermodynamic analysis (FactSage) chart of H_2 reduced pellets.

A preliminary smelting test was performed under an inert (Ar gas) atmosphere. The sample was placed in a graphite crucible and smelted in a resistance furnace. The maximum smelting temperature was 1650 °C with a retention time of 2 h, to ensure efficient separation of Fe. Then the crucible was left to cool overnight in the furnace. Separation of Fe and slag was achieved, while the slag partially self-disintegrated.

Standard leaching tests were performed with the slag produced. The concentration of Na_2CO_3, duration and temperature of the test was the same as in the first approach (section 2.3.1). This time a lower S/L ratio value was selected, corresponding to an excess of leaching agent, in an attempt to maximize the Al extraction, if possible. The experimental conditions are summarized in Table 3.

Table 3. Experimental conditions of produced slag leaching tests after the smelting process.

Duration (h)	6
S/L ratio (%)	5
Na_2CO_3 (wt. %)	8
Excess of H_2 reduced pellets (%)	20
Temperature (°C)	95
Stirring rate (rpm)	300

Accordingly, the liquors and the solid residues were sent for analysis by AAS and ICP required for the calculation of the leaching efficiency and characterization of the leach residue by XRD.

3. Results and Discussion

The results of the experimental work will be presented in the same order as the one followed in the Experimental Methodology section (section 2.3), starting with the "Leaching first/Fe separation second" approach and concluding with the "Fe separation first/Alkaline leaching second" approach. Points meriting attention are discussed in parallel with the presentation of the results.

3.1 "Alkaline Leaching First/Fe Separation Second" Approach

3.1.1 Metal Extraction Results

Al, Si, Ca and Fe extraction yields of the tests conducted with Na_2CO_3, as well as the corresponding Al_2O_3 and SiO_2 equivalent concentration of the resulting aluminate solutions are shown in Figure 5 and Table 4, respectively.

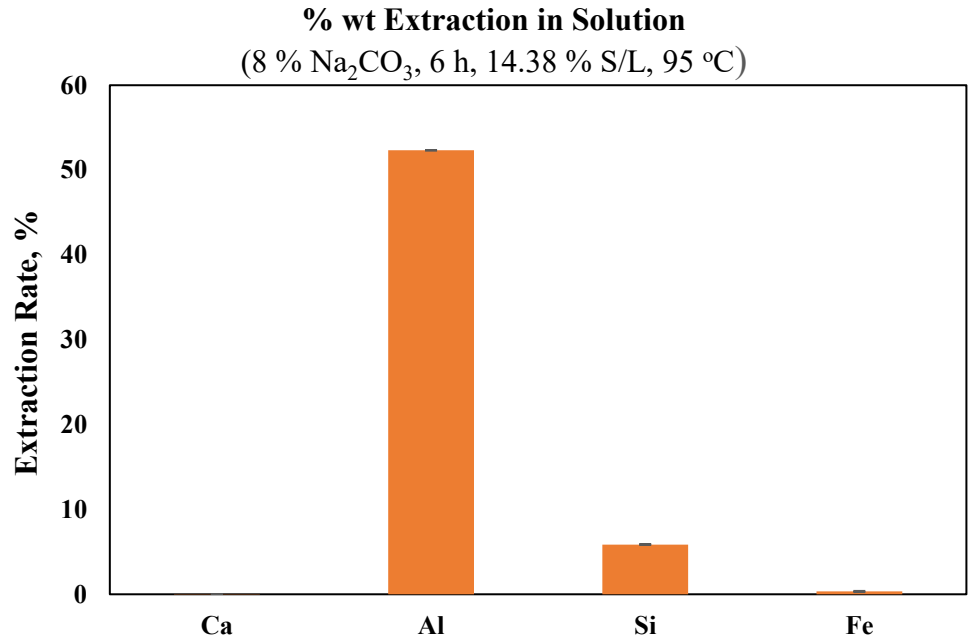

Figure 5. Metal extraction results obtained from the leaching of H_2 reduced BR with Na_2CO_3

Table 4. Metals equivalent oxide concentrations of PLS

Al_2O_3, g/L	SiO_2, g/L	Fe, g/L	Ca, g/L
15.50	0.40	0.003	BDL*

*Below detection limit (< 0.1 ppm)

According to the results, the PLS does not contain Ca as an impurity, while aluminium extraction is equal to 52.33 % w/w. The moderate Al extraction yield is attributed primarily to the gehlenite content of the pellets and secondly to the precipitation of desilication products and katoite. As expected, the co-dissolution of Fe is limited, but still detectable, in the conditions tested. Approximately 30 mg Fe/L is found in the PLS. The Fe content is not a limiting factor for the leaching of the pellets, in the presence of Ca Aluminates. The extraction percentage and concentration of Si observed are in the typical range expected, according to our experience with similar slags, subjected to high temperature leaching processes [14, 16].

3.1.2 Characterization of H_2 Reduced Pellets Leaching Residue

The concentration of total Fe and of the metals of interest Al, Si and Ca (expressed in equivalent oxide basis) is shown below (Table 5). As expected, the residue is predominantly of CaO/Fe composition, with reduced amounts of Al_2O_3 and SiO_2, as expected from the leaching results.

Table 5. Chemical analysis of the H_2 reduced pellets leaching residue

Oxide	Al_2O_3	SiO_2	CaO	Fe Total
Composition (% (w/w))	9.60	6.00	30.20	21.38

According to the particle size analysis results, the H_2 reduced pellets leaching residue, has increased particle size values compared to the initial material, with D(0.5) = 15.46 μm, and D(0.9) = 167.74 μm. The increased particle size values are attributed to the precipitation of $CaCO_3$ on the calcium aluminate particles during the leaching process, with further agglomeration effect, resulting in grain growth.

Finally, the crystallographic analysis of leaching residue (Figure 6) confirms the formation of a desilication product (N-A-S-H), directly related to the decreased Si and Al content. Moreover, some expected Al losses are attributed to the precipitation of katoite. Gehlenite and mayenite traces are also detected, linked to the unleached aluminium, remaining in the system.

According to microstructure analysis of H_2 reduced pellets leaching residue (Figure 7), Fe presents the same behavior as in the initial material presented in Figure 2.

It is observed (Figure 7, images (a) to (f)) that the Fe content is finely distributed and locked in the non-metallic fraction matrix of the leaching residue which has a size range of 0.92–10.2 μm. Thus, Fe separation from the grey mud is a major issue that must be overcome to enhance the process efficiency. Wet magnetic separation was tested as a method for the separation of Fe from the grey mud matrix.

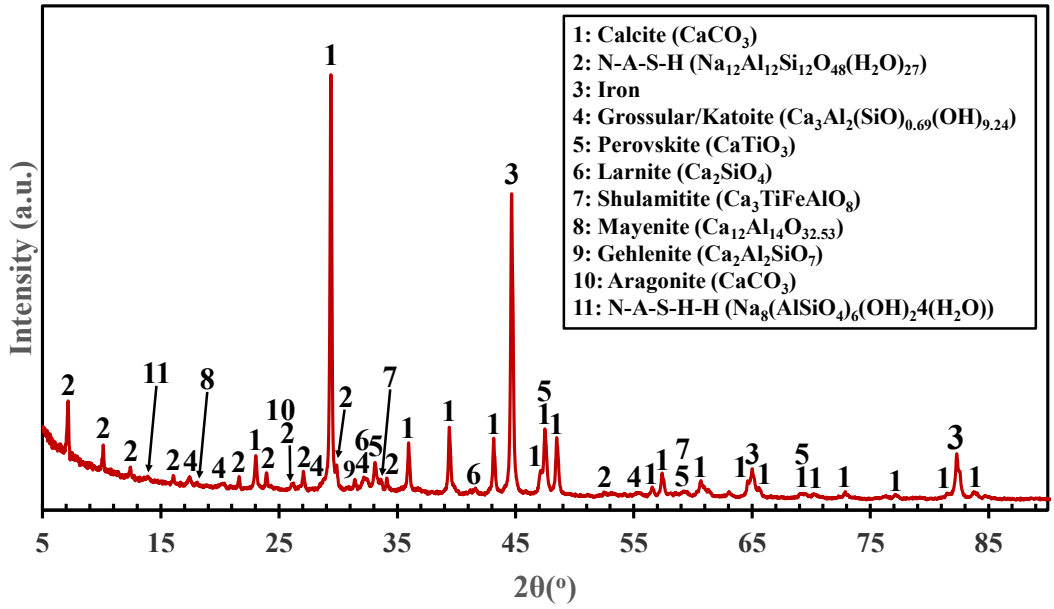

Figure 6. Powder X-Ray Diffractogram and phase identification of the H_2 pellets leaching residue

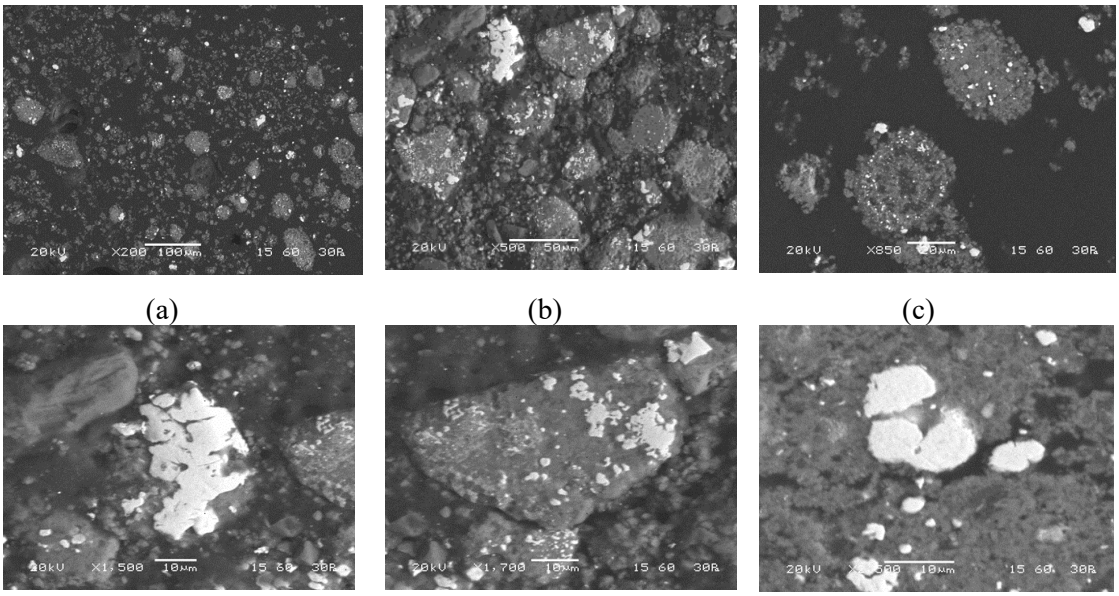

Figure 7. Scanning Electron Microscopy images of H_2 reduced pellets leaching residue at different magnification levels.

3.1.3 Magnetic Separation Test of Leaching Residue (Grey Mud)

The sample of the leaching residue (17 g) was passed through the Magnetic Separator (WHIMS), where an intense magnetic field is generated by two coils. A current intensity of 0.01 A was used, which resulted in a Magnetic Fraction (MAG) equal to 5.08 g and a Nonmagnetic Fraction (NM) equal to 11.04 g. Both fractions were dried at 105 °C for 24 h and characterized by chemical, mineralogical and particle size analysis. The received fractions after the magnetic separation

(termed “NM”-Non-Magnetic and “MAG”-Magnetic) were subjected to chemical, mineralogical and particle size characterization.

The chemical analysis results of the leaching residue after magnetic separation are shown in Table 6 for both the Magnetic (MAG) and Non-Magnetic (NM) clusters.

Table 6. Chemical analysis of the H_2 pellets leaching residue after magnetic separation.

Oxide Composition (% (w/w))	Al_2O_3	SiO_2	CaO	Fe Total
Magnetic Fraction (MAG)	7.20	5.00	27.70	25.10
Non-Magnetic Fraction (NM)	7.21	5.70	28.50	20.47

According to the results, the Fe content after magnetic separation reveals just a slight decrease in Fe as observed in NM cluster, indicating failed separation. Specifically, the total Fe content of NM sample is equal to 20.47 % w/w, in comparison with the initial H_2 reduced pellets residue with a Fe content equal to 21.38 % w/w.

The particle size analysis (Table 7) of MAG and NM clusters was also conducted. The increased particle size values of MAG and NM samples compared to the leaching residue (LR) before the magnetic separation are attributed to the addition of H_2O to create the pulp for the magnetic separation, that leads to aggregation of the residue particles.

Table 7. Particle size analysis of the H_2 pellets leaching residue before and after magnetic separation.

	D(0.5), µm	D(0.9), µm
L.R (before magnetic separation)	15.46	167.74
NM (after magnetic separation)	24.89	354.03
MAG (after magnetic separation)	171.14	598.15

The aforementioned chemical analysis results (Table 6) are also confirmed by crystallographic analysis of MAG and NM fractions (Figure 8), after magnetic separation.

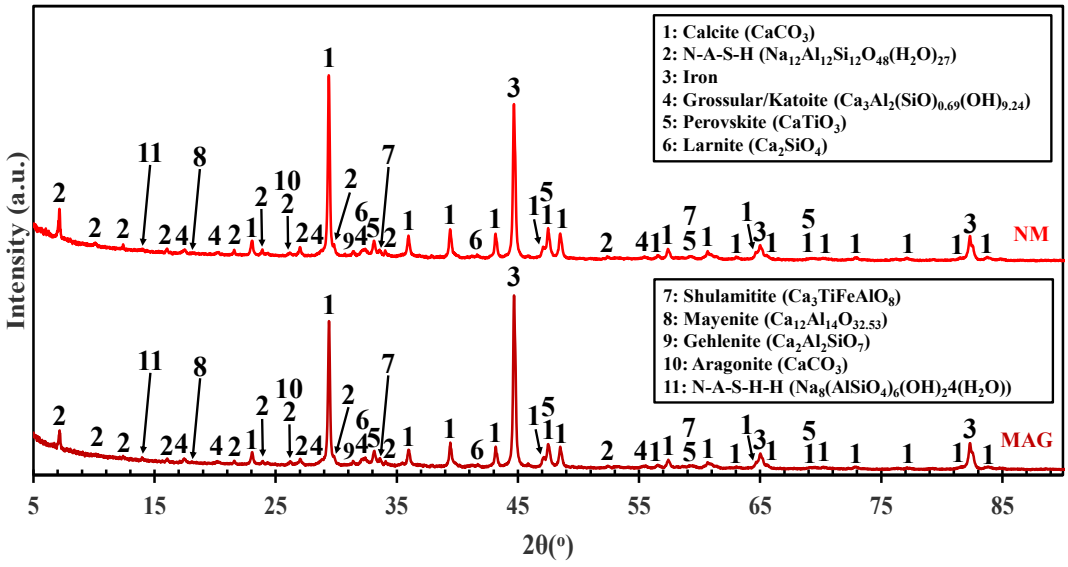

Figure 8. Powder X-Ray Diffractogram and phase identification of the Magnetic (MAG) and Non-Magnetic (NM) H_2 reduced pellets leaching residue after magnetic separation.

As can be seen by Figure 8, Fe is the major phase for both the MAG and NM fractions, with just a slight increase in the intensity of Fe peak in the magnetic sample. However, the iron detected phase after magnetic separation confirms once again the incompatibility of the process, forcing the need for other options to manage the effective Fe separation from the system.

3.2 "Fe Separation First/Alkaline Leaching of Slag Second" Approach

After the unsuccessful separation of Fe observed in the previous experimental approach, (Section 3.1.3), an alternative approach was studied, as mentioned earlier, which aims at separating the Fe with a pyrometallurgical smelting step (Figure 9). Besides the separation of Fe, the smelting stage aims at the formation of a leachable calcium aluminate slag.

According to the results of thermodynamic analysis using FactSage, 60 g amount of ground H_2 pellets was added to a graphite crucible at 1642 °C in a resistance furnace located in Pyrometallurgical Laboratory of Mining and Metallurgical Department at NTUA. After the end of the process, two phases were produced, an iron sample (19.3 g) and a slag that partially self-disintegrated (39.5 g) that was used as raw material for Na_2CO_3 leaching with further evaluation of produced PLS and leaching residue.

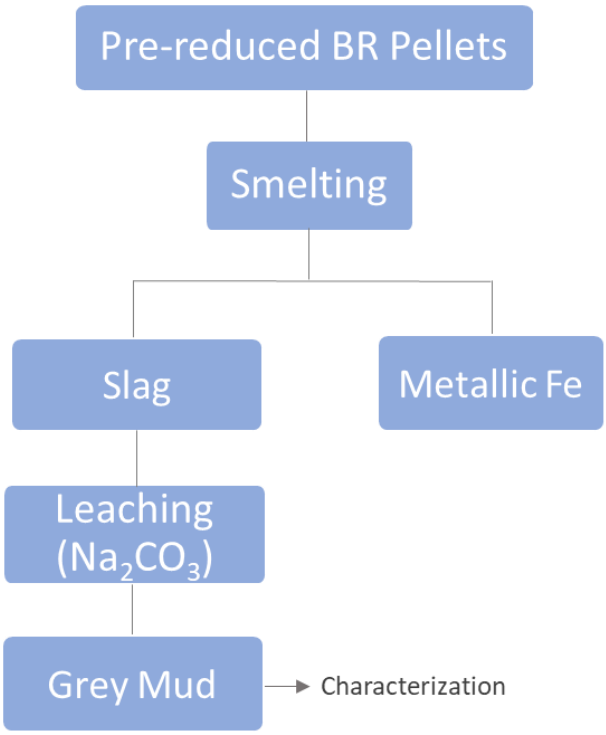

Figure 9. Flowsheet of Fe separation first/Alkaline leaching of slag second approach.

3.2.1 Characterization of the Slag

The slag produced was subjected to chemical analysis (Table 8), revealing higher Al and Ca oxide contents compared to the pre reduced pellets. The iron content was decreased from 23 to 1.4 %, indicating effective Fe separation through the smelting process. The slag was partially self-disintegrating.

The slag was ground (including the self-disintegrated fraction) and a particle size analysis was performed, resulting in a mean particle size of D(0.5) = 7.36 μm and D(0.9) = 45.76 μm.

Table 8. Chemical analysis of produced slag after smelting process.

Oxide	Al_2O_3	SiO_2	CaO	Na_2O	TiO_2	Fe tot.	Others
Composition (% (w/w))	29.8 ± 0.42	10.7 ± 0.01	50.7 ± 0.18	0.2 ± 0.06	5.6 ± 0.02	1.4 ± 0.02	1.60

Mineralogical analysis of the slag produced was also conducted, and the resulting crystalline phases are shown in Figure 10. Pentacalcium trialuminate (C_5A_3) was mainly detected as the leachable aluminate phase and tricalcium aluminate (C_3A) as a non-leachable one. Mayenite was not observed, probably due to inert furnace atmosphere conditions during the smelting and solidification process that prohibited mayenite formation. According to the literature, mayenite formation is favored under O_2 or H_2O atmosphere, instead of Ar that was used in this preliminary melting test [17]. Further optimizations are needed for the formation of an optimum slag, but this work is beyond the scope of the present work.

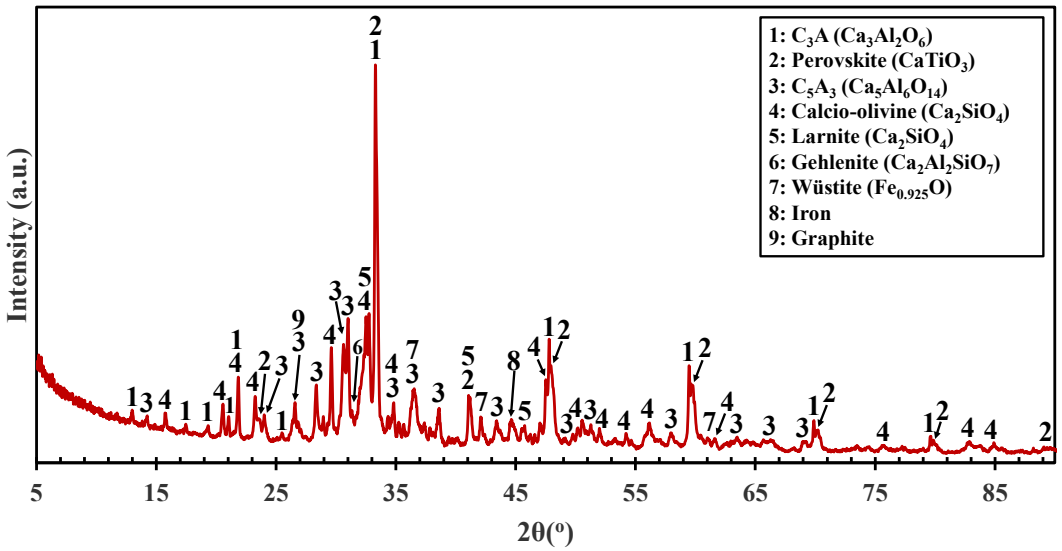

Figure 10. Powder X-Ray Diffractogram and phase identification of the produced slag after melting process.

A quantitative XRD analysis (Table 9) was also performed and confirmed the results of the aforementioned chemical and mineralogical analyses, revealing 31.42 % w/w concentration of C_5A_3 and 19.1 % w/w C_3A respectively. Due to the high C_3A concentration only moderate Al extraction yields are to be expected in the leaching stage, as will be described in the next section (Section 3.2.2).

Table 9. Quantitative XRD analysis of the slag after melting process

Amorphous Content, %	11.87
Larnite, %	13.46
C_3A %	19.10
C_5A_3, %	31.42
Calcio-olivine, %	15.10
Iron, %	0.57
Perovskite, %	6.43
Gehlenite, %	1.08
Wüstite, %	0.49
Graphite, %	0.48

3.2.2 Standard Leaching Test of the Slag and Characterization of the Leaching Residues

Extraction efficiencies for the main metals (Al, Si, Ca and Fe) and metal oxide concentrations of the produced slag's leaching test are presented in Figure 11 and Table 10, respectively. The experimental conditions of this test are extensively described in Table 3 at chapter 2.3.2. A low S/L ratio (5 %) was used in this leaching test due to the limited amount of the slag available after the melting process (39.5 g).

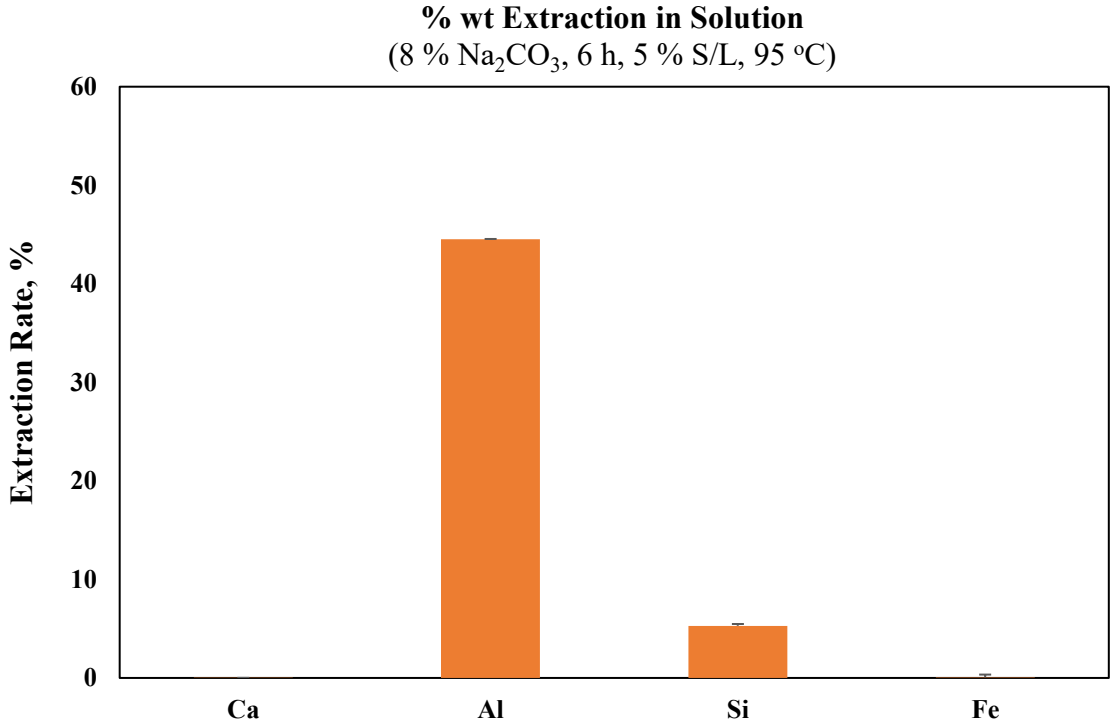

Figure 11. Metal extraction results obtained from the leaching of produced slag with Na_2CO_3.

Table 10. Metals extraction efficiencies and equivalent oxide concentrations in the PLS of produced slag after the smelting process.

Al_2O_3, g/L	SiO_2, g/L	Fe, g/L	Ca, g/L
6.61	0.21	0.0004	BDL*

*Below detection limit (< 0.1 ppm)

According to the results, aluminium extraction is equal to 44.50 % w/w. The moderate Al extraction yield is attributed to the presence of non-leached C_3A and gehlenite. About 0.4 ppm of Fe is detected in PLS, confirming once again the Fe separation efficiency of smelting process. Si concentration of 5.3% w/w is commonly observed in this type of high temperature leaching processes.

The chemical analysis results of slag leaching residue (Table 11) reveal decreased Al and Ca oxide (13.9 % w/w and 40.5 % w/w respectively) concentrations compared to the initial raw material with Al_2O_3: 29.8 % w/w and CaO: 50.7 % w/w. Fe composition remains the same in the residue with a value equal to 1.5 % w/w.

Table 11. Chemical analysis of the slag's leaching residue

Oxide	Al_2O_3	SiO_2	CaO	Fe Total
Composition (% (w/w))	13.90	7.70	40.50	1.5

The particle size analysis of produced slag leaching residue indicated low particle size values compared to the produced slag with D(0.5): 13.48 μm and D(0.9): 149.16 μm. The increased D(0.5) and D(0.9) values are attributed to the particles growth during the leaching process leading to aggregation of the residue particles.

The mineralogical analysis of the produced slag leaching residue is presented in Figure 12.

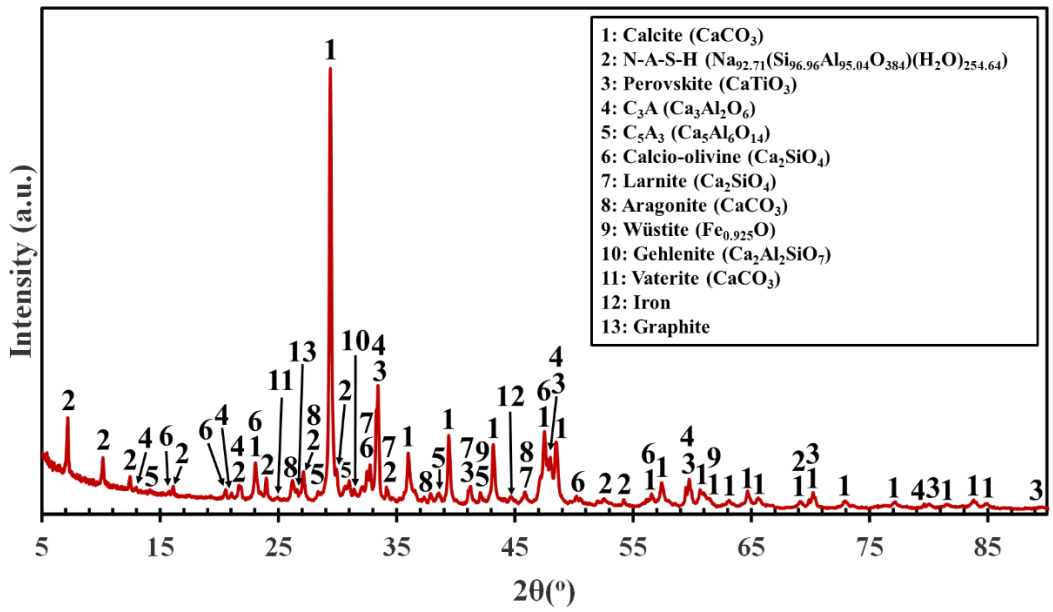

Figure 12. Powder X-Ray Diffractogram and phase identification of the leaching residue using produced slag after smelting process, as raw material.

The mineralogical analysis confirms the leaching results with limited Al content due to the presence of gehlenite and tricalcium aluminium oxide. The main phases in leaching residue are $CaCO_3$ and $CaTiO_3$, while sodium aluminum silicon oxide hydrate is detected as a desilication product in which could be attributed a part of Al losses.

4. Conclusions

The key conclusions from this study are summarized below:

- Hydrogen reduced pellets of BR/CaO mixtures were metallurgically treated for separation of Fe and extraction of Al. Two approaches were studied: (a) "Alkaline leaching first/Fe separation second" and (b) "Fe separation first/Alkaline leaching of slag second".

- The findings of the "Alkaline leaching first/Fe separation second" approach were as follows:
  - i. The moderate Al extraction yield (52.33 %) is attributed primarily to the gehlenite content of H_2 pellets and secondly to the precipitation of desilication product and katoite.
  - ii. Even though the Fe content of the H_2 reduced pellets does not affect the leaching efficiency as long as leachable calcium aluminates are present, it must be removed before further purification processes.

iii. Magnetic separation of the H_2 reduced pellets leaching residue was examined as an option for Fe removal, but this approach proved unsuccessful under the conditions used.

- The findings of the "Fe separation first/Leaching of slag second" approach were as follows:
  i. Smelting of H_2 reduced pellets was tested as a second approach to separate pyrometallurgically the Fe content from the aluminate phases, producing a calcium aluminate slag and metallic Fe.
  ii. After the successful Fe separation via smelting process, the slag (Fe-free) was used as raw material for standard leaching tests indicating low Al extraction efficiency despite Fe removal, due to the presence of C_3A in slag that is unleachable in Na_2CO_3 solutions.

This work showed that the smelting process proved to be a better route for the separation of Fe derived from H_2 reduction of BR. The reason for this is the extremely fine and dispersed particles of Fe that are locked into the oxide matrix and cannot be easily separated. The smelting conditions used are a key factor for the production of a slag with the appropriate mineralogical profile that can be effectively leached and optimized based on the already known experimental protocol.

5. Acknowledgements

This work was carried out in the framework of the H2020 HARARE project. The HARARE project recieves funding from the European Community's Horizon 2020 Programme (H2020/20142020) under grant agreement n°958307 (cordis.europa.eu/project/id/958307).

6. References

1. International Aluminium Institute launches Bauxite Residue Roadmap, https://international-aluminium.org/news-recycling/ (Accessed on 01/08/2024).
2. Ken Evans, The History, challenges, and new developments in the management and use of bauxite residue, *Journal of Sustainable Metallurgy*, Vol. 2 / Issue 4, (2016), 316–331
3. M. Archambo and Surendra Kawatra, Red Mud: Fundamental and New Avenues for utilization, *Mineral Processing and Extractive Metallurgy Revie*w, Vol. 42 / Issue 7, (2021), 427–450
4. M.A. Khairul, Jafar Zanganeh and Behdad Moghtaderi, The composition, recycling, and utilization of Bayer red mud, *Resources, Conservation and Recycling*, Vol. 141, (2019), 483–498
5. Craig Klauber, Markus Gräfea and Greg Power, Bauxite residue issues: II. options for residue utilization. *Hydrometallurgy,* Vol. 108 (2011), 11–32.
6. M. Archambo and Surendra Kawatra, Utilization of bauxite residue: recovering iron values using the iron nugget process, *Mineral Processing and Extractive Metallurgy Revie*w, Vol. 42 / Issue 4, (2021), 222–230
7. Hydrogen As the Reducing Agent in the Recovery of metals and minerals from metallurgical waste; https://h2020harare.eu/ (Accessed on 01/08/2024).
8. RMIS – Raw Material Information System, https://rmis.jrc.ec.europa.eu/?page=environmental-policies-and-regulation-f7695f. (Accessed on 01/08/2024).
9. Michal Ksiazek et al., Iron removal from bauxite ores, *2nd International Bauxite Residue Valorisation and Best Practices Conference*, Athens, Greece, (2018), page 39. ISBN-number: 9789082825923
10. Stacy Gates-Rector and Thomas Blanton, The powder diffraction file: A quality materials characterization database. *Powder Diffraction,* (2019), Vol. 34 / No 4, 352–360.

11. Yuguan Zhang et al., Highly efficient separation of titanium minerals from a modified bauxite residue through direct reduction: A comparison study, *Journal of Materials Research and Technology*, 2023, 26, pp. 6331-6341, ISSN 2238-7854, doi.org/10.1016/j.jmrt.2023.09.017
12. Ganesh Pilla et al., Towards sustainable valorization of bauxite residue: Thermodynamic analysis, comprehensive characterization, and response surface methodology of H_2 reduced products for simultaneous metal recovery, *Journal of Cleaner Production*, 2024, 440, 140931, ISSN 0959-6526, doi.org/10.1016/j.jclepro.2024.140931
13. M.Z. Southard, R.L. Rowley, W.V. Wilding, Densities, D.W. Green, M.Z. Southard (Eds.), *Perry's Chemical Engineers' Handbo*ok (9th edition), McGraw-Hill Education, New York (2019)
14. Eirini Georgala et al., Aluminium extraction from a calcium aluminate slag using sodium carbonate based on the critical examination of the patented industrial Pedersen process, *Hydrometallurgy*, 2023, Vol. 222, 106188, ISSN 0304-386X, doi.org/10.1016/j.hydromet.2023.10618
15. C.W. Bale et al., FactSage thermochemical software and databases, 2010–2016, *Calphad*, 2016, Vol. 54, 35–53
16. Michalis Vafeias et al., Leaching of Ca-rich slags produced from reductive smelting of bauxite residue with Na_2CO_3 solutions for alumina extraction: Lab and pilot scale experiments, *Minerals*, 2021, Vol. 11, 896. https://doi.org/10.3390/min11080896
17. Adamantia Lazou, Liev Kolbeinsen and Jafar Safarian, Evaluation of calcium aluminate slags and pig irons produced from the smelting-reduction of diasporic bauxite, *Materials* 2021, Vol. 14, https://doi.org/10.3390/ma14247740.